Analyzing and modeling the interaction potential of the ground-state beryllium dimer

X. W. Sheng,[1,2,*] X. Y. Kuang,[1,†] P. Li,[1,‡] and K. T. Tang[1,3,§]

[1]*The Institute of Atomic and Molecular Physics, Sichuan University, Chengdu, Sichuan 610065, China*

[2]*Department of Physics, Anhui Normal University, Wuhu, Anhui 241000, China*

[3]*Department of Physics, Pacific Lutheran University, Tacoma, Washington 98447, USA*

(Received 12 November 2012; published 27 August 2013)

The factors that caused the Be_2 potential to be quite different from other conventional van der Waals potentials are quantitatively delineated with relatively simple self-consistent-field calculations. By decomposing the potential into its three major components, we are able to show that the rather sudden change of slope in the potential energy curve around 3.2 Å is the result of the interplay between the *sp* hybridization and the correlation energy. It also enables us to model the interaction with a classical van der Waals potential, which provides the proper long-range behavior of the system, and a short-range attraction which mimics the effects of the *sp* hybridization.

DOI: 10.1103/PhysRevA.88.022517 PACS number(s): 31.15.B−, 31.15.vn, 31.10.+z

I. INTRODUCTION

It has been quite a challenge to determine the beryllium dimer potential. At first even the existence of the beryllium dimer was in question. In 1929, when Herzberg [1] failed to produce Be_2 in his laboratory, he concluded that the interaction between two ground-state beryllium atoms is repulsive. Before the calculations of Liu *et al.* in 1980 [2,3], which showed that Be_2 has a deep minimum (806 cm^{-1}) at a short bond length (2.49 Å), theoretical investigations, including valence bond [4], self-consistent field [5], and configuration interaction [6] calculations, all showed that the Be_2 dimer potential is repulsive. The existence of the beryllium dimer was definitively established in 1984 after the observation of the excitation spectrum of Be_2 by Bondybey *et al.* [7,8]. This motivated another wave of theoretical studies. By now over 100 papers with practically all theoretical methods of quantum chemical calculations have appeared in the literature. Calculations before 1995 were summarized by Røeggen and Almlöf [9]. More recent publications can be found in Ref. [10].

As calculations get more and more sophisticated, the estimated well depths become steadily deeper [11–20], exceeding Bondybey's initial experimental value (790 ± 30 cm^{-1}) by larger and larger amounts. These are complicated calculations because of the small energy separation between the $2s$ and $2p$ orbitals of the beryllium atom, which results in a multiconfigurational ground state. For example, an all-electron full configuration interaction calculation involved more than a billion symmetry-adapted determinants [21].

In 2009, Merritt *et al.* [22] recorded the stimulated emission pumping spectra that sample all the bond vibrational levels of the ground state of beryllium dimer. The well depth D_e (927.7 ± 2.0 cm^{-1}) of the potential energy curve derived from this experiment is in agreement with the high-level quantum chemical estimate (938 ± 15 cm^{-1}) of Patkowski *et al.* [23]. Furthermore, the shape of the experimental potential is very similar to the semiempirical potential obtained by tuning the *ab initio* potential to reproduce experimental spectra [24]. Thus consensus on the ground-state potential of Be_2 has finally been reached.

Diatomic molecules formed from two closed-shell atoms are van der Waals molecules. Dimers of group 2 (alkaline-earth metals), group 12 (battery element), and group 18 (rare-gas) are in this category. It is well known that the binding of van der Waals molecules is mainly due to the dispersion energy. For these dimers, the ground state is only weakly bound with a large equilibrium distance. Apparently this is not the case for the beryllium dimer, although the beryllium atom is a member of the alkaline-earth family.

The long-range behavior of van der Waals molecules should be described by the dispersion series $-C_6/R^6 - C_8/R^8 - C_{10}/R^{10}$, where C_n are known as the dispersion coefficients (or van der Waals coefficients) [25,26]. At large R, where there is no overlap of the two atomic wave functions, the interatomic correlation is given by this dispersion series. At small R, this series must be damped due to the electronic overlap. There are several potential models [27–33] consisting of a hybrid combination of a short-range Born-Mayer potential and a damped dispersion series that can describe all dimers in these families except the beryllium dimer [34]. We shall call potentials that can be described by these models "classical van der Waals potentials."

The Be_2 potential has a unique shape. It has a potential well that is much deeper at a bond length much shorter than that of Mg_2, the heavier neighbor in the alkaline-earth family. This is an anomaly [34]. Strangest of all, the beryllium dimer potential curve has a rather sudden change of slope at about 3.2 Å. This unique potential was described by Merritt *et al.* [22] with an expanded Morse oscillator function. The failure of this function to predict the $v = 11$ state was attributed by Patkowski *et al.* [35] to its lack of proper long-range behavior. The long-range potential is particularly important for collisions of cold atoms, since they are sensitive to that part of the potential [36–38].

The unique shape of the Be_2 potential is due to the small radius of the $1s^2$ core and the near degeneracy of $2s$ and $2p$ energy levels of the beryllium atom. These factors facilitate a

*xwsheng2@163.com
†kuangxiaoyu@scu.edu.cn
‡lpscun@163.com
§tangka@plu.edu

close approach of the beryllium atoms so that sp hybridization can occur to make the Be_2 bond much stronger than usual [39–41].

In this paper, these factors are quantitatively delineated with relatively simple self-consistent-field (SCF) calculations. The Be_2 potential is decomposed into three major components. The attractive energy necessary for bonding is still the correlation energy which can be described by a damped dispersion series, just as in other van der Waals molecules. The change of slope in the potential energy curve is explicitly shown to be the result of the interplay between the correlation energy and the sp hybridization which weakens the usual SCF repulsion. The amounts that the repulsive wall is lowered can be approximated by a smooth function. As a consequence, the beryllium dimer potential can be modeled by a classical van der Waals potential plus a simple short-range attraction.

Atomic units will be used in all calculations. For comparison with literature values, the results are reported in energy units of cm^{-1} and length units of Å. For energy, 1 a.u. = 1 hartree = $2.194\,74 \times 10^5$ cm^{-1}; for distance, 1 a.u. = 1 bohr = 0.529 17 Å; for inverse distance, 1 a.u. = 1.889 75 $Å^{-1}$.

II. METHODOLOGY AND CALCULATION

A. Near degeneracy of 2s and 2p energy levels of the Be atom

Much insight can be gained from comparing the potential energies of helium and beryllium dimers. Both atoms have an outer closed electronic s^2 shell. However, the large differences in magnitude and shape between these two dimer potentials are not what the similarity of the electronic configurations of helium ($1s^2$) and beryllium ($1s^2 2s^2$) atoms would suggest. These differences are caused by the near degeneracy of the 2s and 2p energy levels of the beryllium atom.

First, Stärck and Mayer [13] showed that a small energy difference between the 2s and 2p orbitals of the Be atom results in a considerable enhancement of the dispersion attraction in Be_2. Indeed, the dispersion coefficients of Be_2 [$C_6(Be_2)$ = 214 a.u.] [42] are much larger than that of He_2 [$C_6(He_2)$ = 1.461 a.u.] [43,44]. This makes the Be_2 bond much stronger than the He_2 bond.

In addition, the near degeneracy enables the electrons on the 2s orbital of the Be atom to easily gain access to an entirely empty valence p shell. This sp hybridization will lower the repulsion in Be_2, as predicted by Kutzelnigg [39]. To quantitatively demonstrate this effect, we carried out SCF calculations of the Hartree-Fock energies of both He_2 and Be_2.

The GAMESS(US) package [45] is used for these calculations, and the results are counterpoise corrected [46]. To check convergence, we have used aug-cc-pVDZ, aug-cc-pVTZ, and aug-cc-pVQZ basis sets [47,48]. The differences in results are hardly noticeable. In Fig. 1(a), we show the Hartree-Fock interaction energies of He_2 obtained with only s basis functions (5s) and with a full basis set (5s4p3d2f). In Fig. 1(b), the results with basis functions of (6s), (6s5p), and (6s5p4d3f) for Be_2 are shown. Clearly for He_2, the Hartree-Fock energy calculated with the full basis set is not much different from that with only the s basis function. In contrast, the Hartree-Fock repulsion in Be_2 is greatly reduced when hybridization with p basis functions is possible. As we shall see, this hybridization is the main reason that the shape of the Be_2 potential is so different from the classical van der Waals potential, such as the He_2 potential [49].

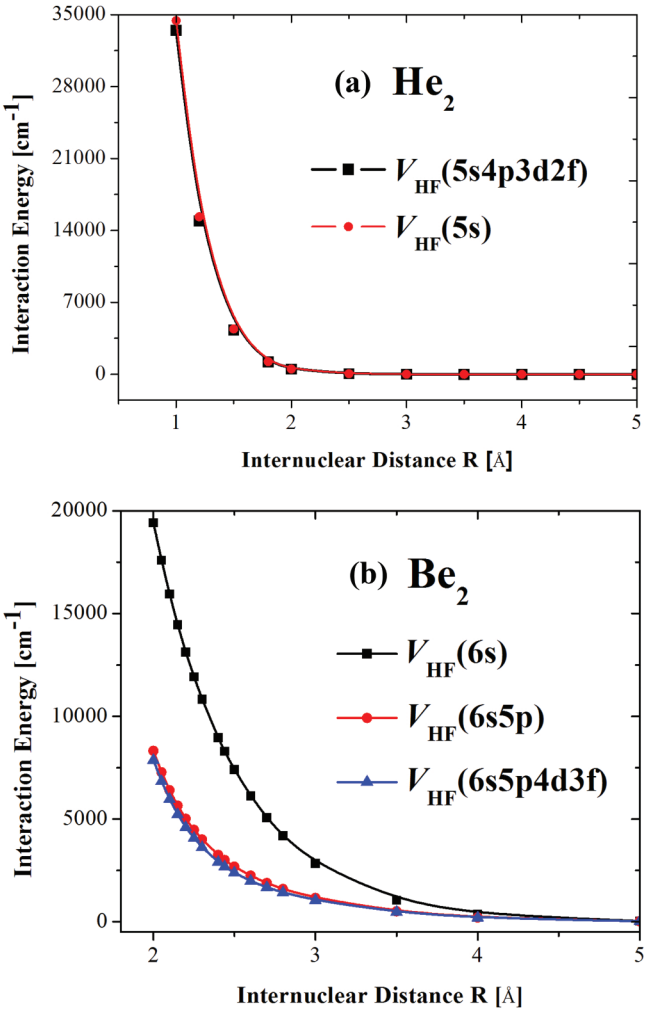

FIG. 1. (Color online) Comparison of Hartree-Fock interaction energies of He_2 and Be_2. For He_2 shown in (a), there is very little difference between the results calculated with the full basis set and with the s basis functions. For Be_2 in (b), the repulsion obtained with s basis functions is greatly reduced by the sp hybridization.

B. Components of the beryllium dimer potential

In the supermolecule approach of the interaction potential, very often the first step is to calculate the Hartree-Fock energy, and the rest is known as correlation energy which is given by the dispersion series in the region of no atomic wave-function overlap. Thus the potential energy $V(R)$ of the beryllium dimer can be written as

$$V(R) = V_{\rm HF}(R) + V_{\rm corr}(R). \quad (1)$$

As seen in the preceding section, it is instructive to separate out the contributions due to the near degeneracy of the 2s and 2p energy levels of the beryllium atom from the Hartree-Fock level interaction energy $V_{\rm HF}(R)$. So we write

$$V_{\rm HF}(R) = V_{\rm HF}^{(s)}(R) + V_{\rm HF}^{(sp)}(R), \quad (2)$$

TABLE I. The ground-state potential of the beryllium dimer and its components.

R (Å)	$V_{\rm HF}$ (cm^{-1})	$V_{\rm HF}^{(s)}$ (cm^{-1})	$V_{\rm HF}^{(sp)}$ (cm^{-1})	$V_{\rm corr}$ (cm^{-1})	$V_{\rm exact}$ (cm^{-1})
2.00	7865.1255	19416.8377	−11551.7122	−6541.2355	1323.8900
2.05	6832.3174	17586.7683	−10754.4509	−6159.3774	672.9400
2.10	5959.5442	15941.3435	−9981.7993	−5789.3262	170.2180
2.15	5221.8515	14460.0149	−9238.1634	−5430.9235	−209.0720
2.20	4597.8259	13124.6643	−8526.8385	−5082.9706	−485.1447
2.25	4069.1508	11919.3092	−7850.1583	−4751.0237	−681.8729
2.30	3620.2157	10829.8502	−7209.6344	−4433.8410	−831.6253
2.40	2910.6182	8950.3534	−6039.7452	−3844.8023	−934.1841
2.44	2682.3292	8295.6466	−5613.3173	−3626.1638	−943.8346
2.50	2386.0862	7403.4291	−5017.3429	−3316.4173	−930.3311
2.60	1988.5489	6124.7997	−4136.2507	−2848.8072	−860.2583
2.70	1678.2604	5064.5090	−3386.2487	−2441.4495	−763.1891
2.80	1428.6310	4183.4397	−2754.8088	−2091.5068	−662.8758
3.00	1047.7980	2841.1830	−1793.3850	−1541.8158	−494.0178
3.50	471.9416	1043.0821	−571.1405	−759.2863	−287.3447
4.00	193.3492	364.1936	−170.8444	−396.9232	−203.5740
5.00	25.2165	38.4984	−13.2819	−112.4395	−87.2230
6.00	2.6060	3.5279	−0.9219	−34.1294	−31.5234
7.00	0.2283	0.3184	−0.0900	−12.0266	−11.7983
8.00	0.0176	0.0301	−0.0125	−4.9655	−4.9479

where $V_{\rm HF}^{(s)}(R)$ is the Hartree-Fock level energy calculated with only s basis functions. That is, if $E_{{\rm HF}(s)}^{{\rm Be}_2}(R)$ is the Hartree-Fock energy calculated with only s basis functions as described in the preceding section, then

$$V_{\rm HF}^{(s)}(R) = E_{{\rm HF}(s)}^{{\rm Be}_2}(R) - 2E_{{\rm HF}(s)}^{\rm Be}.$$

Therefore, $V_{\rm HF}^{(sp)}(R)$ represents the energy coming from the hybridization of the s and p atomic orbitals in the beryllium atom and can be evaluated by the difference of $V_{\rm HF}(R)$ and $V_{\rm HF}^{(s)}(R)$ [$V_{\rm HF}^{(sp)}(R) = V_{\rm HF}(R) - V_{\rm HF}^{(s)}(R)$]. It follows that

$$V(R) = V_{\rm HF}^{(s)}(R) + V_{\rm HF}^{(sp)}(R) + V_{\rm corr}(R). \tag{3}$$

In our analysis, we take the nonrelativistic *ab initio* results calculated by Patkowski *et al.* [23,50] as the exact potential $V(R)$. This potential recovers the measured vibrational energies with a root-mean-square error of only 3.4 cm^{-1} and supports the presence of a 12th vibrational level. All their *ab initio* data points are listed in the last column of Table I as $V_{\rm exact}$. These calculations are of course not exact, but for convenience, we use the symbol $V_{\rm exact}$ to refer to these high-quality benchmark results. We have calculated $V_{\rm HF}(R)$ and $V_{\rm HF}^{(s)}(R)$ as described in the preceding section. Their numerical values together with $V_{\rm HF}^{(sp)}(R)$ and $V_{\rm corr}(R)$ [from $V_{\rm exact}(R) - V_{\rm HF}(R)$] are also listed in Table I.

III. RESULTS AND DISCUSSION

A. Change of slope in the potential energy curve

Based on the numerical values in Table I, $V_{\rm HF}^{(s)}(R)$, $V_{\rm HF}^{(sp)}(R)$, and $V_{\rm corr}(R)$ together with $V(R)$ are shown in Fig. 2. It is clear from Eq. (1) that the bonding of the dimer comes entirely from the attractive correlation energy $V_{\rm corr}(R)$. But the sp hybridization lowers the repulsive potential wall. This effect is represented by $V_{\rm HF}^{(sp)}(R)$, which behaves like a short-range attractive potential. It is practically equal to zero for R greater than 5 Å. After its onset, it rapidly becomes more negative as R decreases. It intersects the long-range correlation energy $V_{\rm corr}(R)$ at 3.2 Å. For $R \gg 3.2$ Å, $V_{\rm corr}(R)$ dominates, and for $R \ll 3.2$ Å, $V_{\rm HF}^{(sp)}(R)$ dominates. Therefore, the sum of these two terms will be closer to $V_{\rm corr}(R)$ for $R > 3.2$ Å, and for $R < 3.2$ Å the sum will be closer to $V_{\rm HF}^{(sp)}(R)$. Since the R dependences of $V_{\rm HF}^{(sp)}(R)$ and $V_{\rm corr}(R)$ are characteristically different, this results in a change of slope in the potential energy curve $V(R)$. Eventually, the sum of these two negative

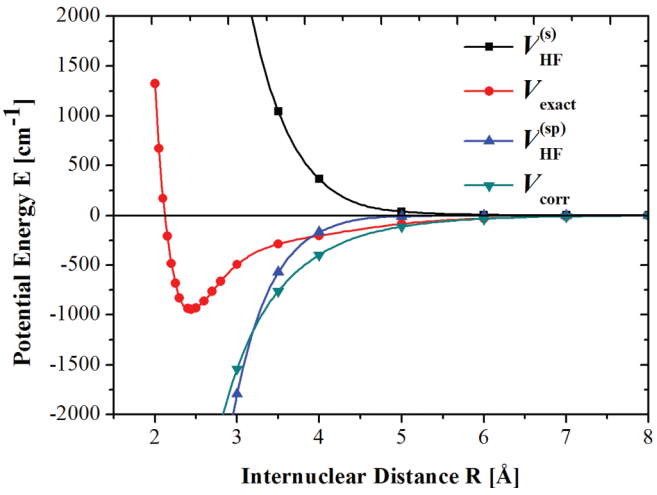

FIG. 2. (Color online) The potential energy curve of the ground state of Be_2 and its components. The intersection of correlation energy $V_{\rm corr}$ and the energy due to sp hybridization $V_{\rm HF}^{(sp)}$ is the main reason for the change of slope in the potential energy curve around 3.2 Å.

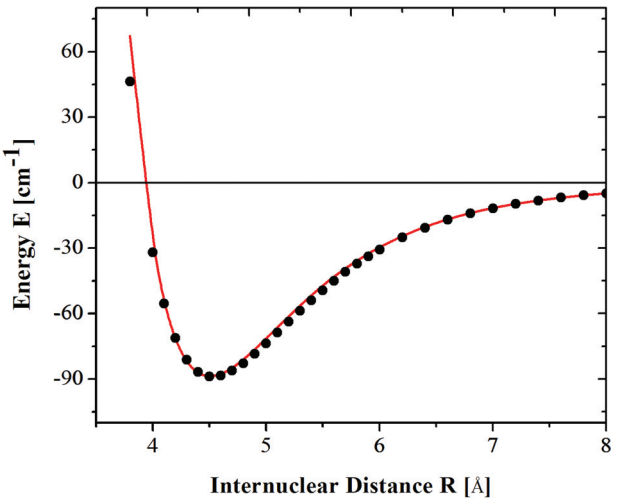

FIG. 3. (Color online) The van der Waals interaction in the Be_2 potential. The dots are the Be_2 potential without the sp hybridization, and the solid line is the Tang-Toennies model for van der Waals potential, determined without adjustable parameters.

terms is overcome by the positive repulsive potential $V_{\rm HF}^{(s)}(R)$ to form a potential well as shown in Fig. 2.

B. Modeling the beryllium dimer potential

It is possible to individually model the three components. However, to clarify the relationship between the classical van der Waals potential and the beryllium dimer potential, we first make the following observation.

In the van der Waals molecule He_2, the sp hybridization effect is negligibly small. The Hartree-Fock energy is essentially the same as $V_{\rm HF}^{(s)}(R)$, as we see in Fig. 1(a). In that case, the total interaction energy, which is almost identical to $V_{\rm HF}^{(s)}(R) + V_{\rm corr}(R)$, can be described by a classical van der Waals potential. This suggests that for beryllium dimer, $V_{\rm HF}^{(s)}(R) + V_{\rm corr}(R)$ may also be similarly modeled. This is indeed the case. In Fig. 3, we show a van der Waals potential, defined as

$$V_{\rm vdW}(R) = V_{\rm HF}^{(s)}(R) + V_{\rm corr}(R), \tag{4}$$

where $V_{\rm HF}^{(s)}(R)$ and $V_{\rm corr}(R)$ are from Table I. The dots are the numerical data and the solid line is a classical van der Waals potential known as the Tang and Toennies (TT) model potential (see below).

In 1984, Tang and Toennies [51] found that the potential consists of the sum of the short-range repulsive Born-Mayer potential $A\exp(-bR)$, and the long-range attractive potential of damped asymptotic dispersion series,

$$V_{\rm TT}(R) = Ae^{-bR} - \sum_{n=3}^{8}\left(1 - e^{-bR}\sum_{k=0}^{2n}\frac{(bR)^k}{k!}\right)\frac{C_{2n}}{R^{2n}}, \tag{5}$$

could describe nearly perfectly the van der Waals potentials for different types of systems such as the triplet state of H_2, the van der Waals dimers He_2 and Ar_2, as well as the van der Waals molecules with open-shell atoms NaAr and LiHg. This equation has been shown to have a firm foundation in the generalized Heitler-London theory [52]. It is now known as the TT potential.

Since Eq. (5) is derived from a physical model [51], it is not surprising that it has predictive power. With accurate dispersion coefficients, the different shapes of many van der Waals potentials have been correctly predicted [34,53]. So far among the systems examined, the only exception is the beryllium dimer potential [34]. To find out why it fails in the case of Be_2 is one of the main objectives of the present study.

The first three dispersion coefficients C_{2n} for many systems can be predicted theoretically with a high degree of accuracy, and higher coefficients can be generated from the recurrence relation [54]

$$C_{2n} = \left(\frac{C_{2n-2}}{C_{2n-4}}\right)^4 C_{2n-6}. \tag{6}$$

Equation (5) depends essentially on only two parameters A and b. Conversely, the potential curve can also be uniquely determined if the well minimum R_e and the well depth D_e are known. There is a simple program in the Appendix of Ref. [55] which, with a given set of C_{2n}, will automatically convert R_e and D_e into A and b.

For Be_2, the first three dispersion coefficients ($C_6 = 214$ a.u., $C_8 = 10\,230$ a.u., and $C_{10} = 504\,300$ a.u.) are accurately determined by Porsev and Derevianko [42]. The well minimum $R_e = 4.5$ Å (8.504 a.u.) and the well depth $D_e = 89.07\ {\rm cm}^{-1}$(0.000 406 a.u.) can also be pinpointed from the data shown in Fig. 3. The Born-Mayer parameters A and b calculated with the program in the Appendix of Ref. [55] are $A = 21.7721$ a.u. and $b = 1.2415$ a.u. The TT potential calculated with these parameters is shown in Fig. 3 as a solid line. Note that this TT potential is constructed with no free parameter, yet it can accurately describe the van der Waals potential of Eq. (4) in the potential well and the long-range region. This clearly shows that the Be_2 potential has van der Waals long-range behavior.

Recently, we have shown that the potentials of all alkaline-earth dimers can be described by the TT potential model [56–58] except for the Be_2 potential [34]. The reason for this exception is now clear. If there were no sp hybridization, the Be_2 potential could also be modeled by the TT potential.

Now to model the entire Be_2 ground-state potential, we must describe the difference $V_d(R)$ between $V(R)$ and $V_{\rm TT}(R)$,

$$V_d(R) = V(R) - V_{\rm TT}(R). \tag{7}$$

With $V(R)$ taken from the last column ($V_{\rm exact}$) of Table I and $V_{\rm TT}(R)$ calculated from Eq. (5), the difference is a smooth function and can be closely fitted with a three-parameter exponential function

$$V_d(R) = De^{-eR-fR^2}, \tag{8}$$

where $D = -4.3224$ a.u., $e = 0.5891$ a.u., and $f = 0.0774$ a.u. The origin of this function is due to the sp hybridization, but it is very close to $V_{\rm HF}^{(sp)}(R)$ only for $R > 3.5$ Å. From that point on down, as R decreases, the difference between $V_d(R)$ and $V_{\rm HF}^{(sp)}(R)$ starts to increase. This is because $V_{\rm TT}(R)$ is too hard in the inner repulsive region [59]. However, since the deviation caused by the inaccuracy of $V_{\rm TT}(R)$ in the inner region is taken into account in $V_d(R)$, the sum of $V_{\rm TT}(R)$

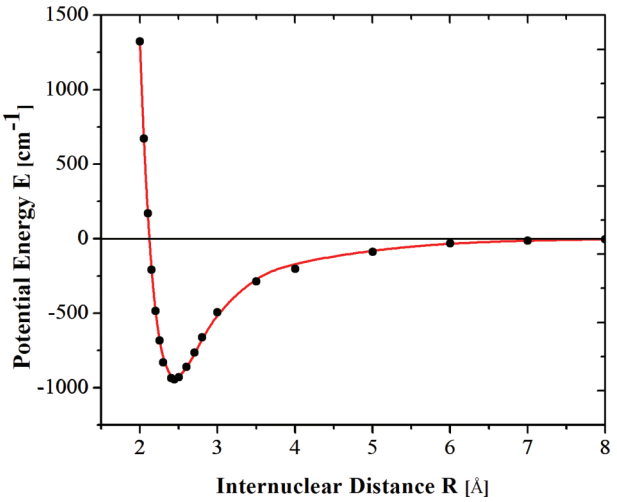

FIG. 4. (Color online) The ground-state potential of the beryllium dimer. The dots are the *ab initio* results calculated by Patkowski *et al.* (Refs. [23] and [50]), and the solid line is generated with the present model.

and $V_d(R)$,

$$V(R) = Ae^{-bR} - \sum_{n=3}^{8}\left(1 - e^{-bR}\sum_{k=0}^{2n}\frac{(bR)^k}{k!}\right)\frac{C_{2n}}{R^{2n}} + De^{-eR-fR^2}, \quad (9)$$

should still be a good description of the Be_2 dimer potential. In Eq. (9), only three parameters (D,e,f) are obtained from fitting [through Eq. (8)]; all other parameters are predetermined. The potential energy calculated from Eq. (9) is shown in Fig. 4 as a solid line. The exact *ab initio* data points are shown as dots. The agreement is clearly seen.

Finally, we should mention that the Be_2 ground-state potential was also successfully modeled by Patkowski *et al.* [35] with a modified TT potential which has eight free parameters in addition to the three dispersion coefficients. These parameters are determined by fitting them to their calculated *ab initio* points. In contrast, our model has only three free parameters. It also seems to us that the physics of our model is more transparent, since every term in our model is associated with some definite meaning.

IV. CONCLUSION

The determinations of the beryllium dimer potential are a great success stories of modern quantum chemistry and laser spectroscopy. In our attempt to understand the strange shape of this potential, we find that the conventional van der Waals interaction theory is still relevant to this case. By decomposing the potential into its three major components, we are able to show that the change of the slope in the potential energy curve around 3.2 Å is the result of the interplay between the *sp* hybridization and the correlation energy. It also enables us to model the entire interaction by a classical van der Waals potential plus a smooth short-range attraction. The classical van der Waals potential, of which the physics is clear, provides the proper long-range behavior of the system, which is important for cold atom physics. The short-range attraction of Eq. (8) mimics the *sp* hybridization effects, which make the Be_2 molecule unique. While all other alkaline-earth dimer potentials can be described by the TT model [34], for Be_2 it is necessary to include this extra term [as in Eq. (9)] for the description of its interaction potential.

ACKNOWLEDGMENTS

We would like to thank Konrad Patkowski for sending us his *ab initio* results of the beryllium dimer potential. X.W. would like to thank Evert Jan Baerends and Łukasz Mentel for helpful discussions about this project. This work is supported by the National Natural Science Foundation of China (Grants No. 11274235 and No. 11104190) and the Doctoral Education Fund of Education Ministry of China (Grants No. 20100181110086 and No. 20111223070653).

[1] G. Herzberg, Z. Phys. **57**, 601 (1929); **84**, 571 (1933).
[2] B. Liu and A. D. Mclean, J. Chem. Phys. **72**, 3418 (1980).
[3] B. H. Lengsfield III, A. D. Mclean, M. Yoshimine, and B. Liu, J. Chem. Phys. **79**, 1891 (1983).
[4] J. H. Bartlett, Jr. and W. H. Furry, Phys. Rev. **38**, 1615 (1931).
[5] S. Fraga and B. J. Ransil, J. Chem. Phys. **35**, 669 (1961); **36**, 1127 (1962).
[6] C. F. Bender and E. R. Davidson, J. Chem. Phys. **47**, 4972 (1969).
[7] V. E. Bondybey and J. H. English, J. Chem. Phys. **80**, 568 (1984).
[8] V. E. Bondybey, Chem. Phys. Lett. **109**, 436 (1984); Science **227**, 125 (1985).
[9] I. Røeggen and J. Almlöf, Int. J. Quantum Chem. **60**, 453 (1996).
[10] A. V. Mitin, Int. J. Quantum Chem. **111**, 2560 (2011).
[11] G. A. Petersson and W. A. Shirley, Chem. Phys. Lett. **160**, 494 (1989).
[12] S. Evangelisti, G. L. Bendazzoli, and L. Gagliardi, Chem. Phys. **185**, 47 (1994).
[13] J. Stärck and W. Meyer, Chem. Phys. Lett. **258**, 421 (1996).
[14] D. Begue, M. Merawa, M. Rerat, and C. Pouchan, Chem. Phys. Lett. **301**, 43 (1999).
[15] J. M. L. Martin, Chem. Phys. Lett. **303**, 399 (1999).
[16] L. A. Kaledin, A. L. Kaledin, M. C. Heaven, and V. E. Bondybey, J. Mol. Struct. (THEOCHEM) **461**, 177 (1999).
[17] R. J. Gdanitz, Chem. Phys. Lett. **312**, 578 (1999).
[18] K. B. Martin, A. K. Leonid, L. K. Alexey, C. H. Michael, and E. B. Vladimir, Chem. Phys. **262**, 15 (2000).
[19] I. Røeggen and L. Veseth, Int. J. Quantum Chem. **101**, 201 (2005).
[20] J. A. W. Harkless and K. K. Irikura, Int. J. Quantum Chem. **106**, 2373 (2006).
[21] S. Evangelisti, G. L. Bendazzoli, R. Ansaloni, F. Duri, and E. Rossi, Chem. Phys. Lett. **252**, 437 (1996).
[22] J. M. Merritt, V. E. Bondybey, and M. C. Heaven, Science **324**, 1548 (2009).

[23] K. Patkowski, R. Podeszwa, and K. Szalewicz, J. Phys. Chem. A **111**, 12822 (2007).
[24] V. Spirko, J. Mol. Spectrosc. **253**, 268 (2006).
[25] A. J. Stone, *The Theory of Intermolecular Forces* (Clarendon, Oxford, 1996).
[26] A. J. Thakkar, in *Encyclopedia of Chemical Physics and Physical Chemistry: Vol. 1 Fundamentals*, edited by J. H. Moore and N. D. Spencer (Institute of Physics, London, 2001), p. 161.
[27] K. T. Tang and J. P. Toennies, J. Chem. Phys. **66**, 1496 (1977).
[28] R. Ahlrichs, R. Penco, and G. Scoles, Chem. Phys. **19**, 119 (1977).
[29] K. C. Ng, W. J. Meath, and A. R. Allnatt, Chem. Phys. **32**, 175 (1878).
[30] R. A. Aziz, Mol. Phys. **38**, 177 (1979).
[31] C. Douketis, G. Scoles, S. Marchetti, M. Zen, and A. J. Thakkar, J. Chem. Phys. **76**, 3057 (1982).
[32] R. R. Fuchs, F. R. W. McCourt, A. J. Thakkar, and F. Grein, J. Phys. Chem. **88**, 2036 (1984).
[33] R. J. Le Roy, C. C. Haugen, J. Tao, and H. Li, Mol. Phys. **109**, 435 (2011).
[34] P. Li, J. Ren, N. Niu, and K. T. Tang, J. Phys. Chem. A **115**, 6927 (2011).
[35] K. Patkowski, V. Špirko, and K. Szalewicz, Science **326**, 1382 (2009).
[36] V. Špirko, S. P. A. Sauer, and K. Szalewicz, Phys. Rev. A **87**, 012510 (2013).
[37] K. M. Jones, E. Tiesinga, P. D. Lou, and P. S. Julienne, Rev. Mod. Phys. **78**, 483 (2006).
[38] W. C. Stwalley and H. Wang, J. Mol. Spectrosc. **195**, 194 (1999).
[39] W. Kutzelnigg, in *Theoretical Models of Chemical Bonding*, edited by Z. B. Maksic (Springer-Verlag, Berlin, 1990), Pt. 2, pp. 1–43.
[40] M. W. Schmidt, J. Ivanic, and K. Ruedenberg, J. Phys. Chem. A **114**, 8687 (2010).
[41] M. C. Heaven, V. E. Bondybey, J. M. Merritt, and A. L. Kaledin, Chem. Phys. Lett. **506**, 1 (2011).
[42] S. G. Porsev and A. Derevianko, J. Exp. Theor. Phys. **102**, 195 (2006).
[43] K. T. Tang and M. Karplus, Phys. Rev. **171**, 70 (1968).
[44] Z. C. Yan, J. F. Babb, A. Dalgarno, and G. W. F. Drake, Phys. Rev. A **54**, 2824 (1996).
[45] M. W. Schmidt, K. K. Baldridge, J. A. Boatz, S. T. Elbert, M. S. Gordon, J. H. Jensen, S. Kosekt, N. Matsunaga, K. A. Nguyen, S. J. Su, T. L. Windus, M. Dupuis, and J. A. Montgomery, J. Comput. Chem. **14**, 1347 (1993).
[46] F. Boys and F. Bernard, Mol. Phys. **19**, 553 (1970).
[47] T. H. Dunning, J. Chem. Phys. **90**, 1007 (1989).
[48] R. A. Kendall, T. H. Dunning, and R. J. Harrison, J. Chem. Phys. **96**, 6796 (1992).
[49] K. T. Tang, J. P. Toennies, and C. L. Yiu, Phys. Rev. Lett. **74**, 1546 (1995).
[50] K. Patkowski (private communication).
[51] K. T. Tang and J. P. Toennies, J. Chem. Phys. **80**, 3726 (1984).
[52] K. T. Tang, J. P. Toennies, and C. L. Yiu, Int. Rev. Phys. Chem. **17**, 363 (1998).
[53] K. T. Tang and J. P. Toennies, J. Chem. Phys. **118**, 4976 (2003).
[54] K. T. Tang and J. P. Toennies, J. Chem. Phys. **68**, 5501 (1978).
[55] K. T. Tang and J. P. Toennies, Z. Phys. D **1**, 91 (1986).
[56] P. Li, W. Xie, and K. T. Tang, J. Chem. Phys. **133**, 084308 (2010).
[57] D. D. Yang, P. Li, and K. T. Tang, J. Chem. Phys. **131**, 154301 (2009).
[58] G. P. Yin, P. Li, and K. T. Tang, J. Chem. Phys. **132**, 074303 (2010).
[59] R. Aziz, A. Dramtz, and M. Slaman, Z. Phys. D **21**, 251 (1991).